

Macro-dipoles in soft/hard expanded-polytetrafluoroethylene + fluoroethylenepropylene (ePTFE + FEP) fluoropolymer-film systems for high-output piezoelectric ferroelectret-transducer applications

Wang, Ningzhen; Baferani, Mohamadreza Arab; Daniels, Robert; Wu, Chao; Huo, Jindong; van Turnhout, Jan; Sotzing, Gregory A.; Gerhard, Reimund; Cao, Yang

DO

10.1088/1361-6463/ad1a84

Publication date 2024

Document VersionFinal published version

Published in

Journal of Physics D: Applied Physics

Citation (APA)

Wang, N., Baferani, M. A., Daniels, R., Wu, C., Huo, J., van Turnhout, J., Sotzing, G. A., Gerhard, R., & Cao, Y. (2024). Macro-dipoles in soft/hard expanded-polytetrafluoroethylene + fluoroethylenepropylene (ePTFE + FEP) fluoropolymer-film systems for high-output piezoelectric ferroelectret-transducer applications. *Journal of Physics D: Applied Physics*, *57*(14), Article 145502. https://doi.org/10.1088/1361-6463/ad1a84

Important note

To cite this publication, please use the final published version (if applicable). Please check the document version above.

Copyright

Other than for strictly personal use, it is not permitted to download, forward or distribute the text or part of it, without the consent of the author(s) and/or copyright holder(s), unless the work is under an open content license such as Creative Commons.

Takedown policy

Please contact us and provide details if you believe this document breaches copyrights. We will remove access to the work immediately and investigate your claim.

Green Open Access added to TU Delft Institutional Repository 'You share, we take care!' - Taverne project

https://www.openaccess.nl/en/you-share-we-take-care

Otherwise as indicated in the copyright section: the publisher is the copyright holder of this work and the author uses the Dutch legislation to make this work public.

PAPER

Macro-dipoles in soft/hard expandedpolytetrafluoroethylene + fluoroethylenepropylene (ePTFE + FEP) fluoropolymer-film systems for high-output piezoelectric ferroelectret-transducer applications

To cite this article: Ningzhen Wang et al 2024 J. Phys. D: Appl. Phys. 57 145502

View the article online for updates and enhancements.

You may also like

- Novel phosphate-grafted ePTFE copolymers for optimum in vitro mineralization
- Edeline Wentrup-Byrne, Shuko Suzuki, Juthakarn Jessica Suwanasilp et al.
- Structural Mechanics Analysis of Woven Web Reinforced Membranes in Proton Exchange Membrane Water Electrolysis Julian Kink, Martin Ise, Boris Bensmann et al
- Comprehensive feasibility evaluation of small-diameter 3D templated vascular graft via physical characterizations and invivo experiments

Sandeep Karna, Ji Eun Lee, Yeong Seo Kim et al.



Macro-dipoles in soft/hard expanded-polytetrafluoroethylene + fluoroethylenepropylene (ePTFE + FEP) fluoropolymer-film systems for high-output piezoelectric ferroelectret-transducer applications

Ningzhen Wang^{1,2,*}, Mohamadreza Arab Baferani², Robert Daniels³, Chao Wu², Jindong Huo², Jan van Turnhout⁴, Gregory A Sotzing³, Reimund Gerhard⁵ and Yang Cao^{2,*}

E-mail: ningzhenwang@bjfu.edu.cn and yang.cao@uconn.edu

Received 28 September 2023, revised 23 December 2023 Accepted for publication 3 January 2024 Published 11 January 2024



Abstract

Multi-layer ferroelectrets consisting of fluoroethylenepropylene (FEP) copolymer and open-porous expanded polytetrafluoroethylene (ePTFE) films exhibit stable internal electret charges, high piezoelectric coefficients and heat resistance, making them promising candidates for wearable sensors or nanogenerators in body-area networks. Here, three- and five-layer (FEP/ePTFE/FEP and FEP/ePTFE/FEP/ePTFE/FEP) ferroelectret stacks were laminated and poled in a corona discharge. The resulting charge distributions were measured by use of the pulsed electro-acoustic (PEA) method and revealed that charges of opposite polarity were trapped at the interfaces between the FEP and ePTFE layers. Thus, the existence of one macro-dipole in the three-layer structure and of two macro-dipoles in the five-layer structure was directly shown for the first time. Moreover, electric-displacement-*versus*-electric-field (D-E) loops revealed that remnant polarization is given by the number of macro-dipoles in the respective stack. Due to the addition of the macro-dipoles, the piezoelectric d_{33} coefficient of the FEP/ePTFE/FEP/ePTFE/FEP stack reaches 200 pC/N even under a potentially non-uniform compression of the soft ePTFE layers. The results should be useful for a better understanding and a performance optimization of ferroelectrets in self-powered intelligent devices.

¹ School of Technology, Beijing Forestry University, Beijing 100083, People's Republic of China

² Electrical Insulation Research Center, Institute of Materials Science, University of Connecticut, Storrs, CT 06269, United States of America

³ Department of Chemistry, University of Connecticut, Storrs, CT 06269, United States of America

⁴ Department of Materials Science and Engineering, Delft University of Technology, Delft, The Netherlands

⁵ Institute of Physics and Astronomy, Faculty of Science, University of Potsdam, Potsdam-Golm 14476, Germany

^{*} Authors to whom any correspondence should be addressed.

Keywords: ePTFE + FEP ferroelectret, charge distribution, piezoelectricity, charge-spring model

1. Introduction

Self-powered and wearable piezoelectric nanogenerators (PENGs) that can harvest abundant mechanical energy from human motions while also monitoring various vital signs have attracted strong research interest in recent years [1–3]. Direct contact with human skin requires the PENG or sensor materials to be biocompatible, flexible and durable, and to exhibit high electromechanical coupling coefficients [2, 4, 5]. Ferroelectrets are piezoelectric polymer foams or film systems with internal cavities that represent electric macro-dipoles after poling in micro-plasma discharges under high external electric fields [6-8]. Compared to piezoelectric ceramics, e.g. lead zirconate titanate (PZT), barium titanate (BaTiO₃), etc [2] or ferroelectric polymers, e.g. polyvinylidene fluoride (PVDF) and some copolymers, etc [9], ferroelectrets combine high piezoelectric d_{33} coefficients with good flexibility [10– 12], and are therefore very suitable for wearable electronics [11].

A range of ferroelectrets that are based on cellularfoam polypropylene (PP) [13, 14], polyethylene (PE) [15, 16], cyclo-olefin copolymers (COCs) [17], polycarbonate (PC) [14], fluoroethylenepropylene (FEP) copolymers [18, 19], sandwiched FEP films or porous polytetrafluoroethylene (PTFE), etc [20], have been developed. There are three main types of internal porous structures following from different fabrication processes: (1) closed lens-shaped pores, as in PP [13], PE [15] and FEP [14] ferroelectrets can be generated by inflating the respective polymer under high-pressure nitrogen or carbon-dioxide gas before heat treatment; charges of opposite polarity are trapped on opposite inner surfaces after poling. Piezoelectricity occurs when the dipole moments in the pores change. (2) Artificial cavities can be designed to act as macropores after being charged, e.g. parallel channels in FEP ferroelectrets prepared around templates [18, 19], COC ferroelectrets with laser-cut rectangular channel arrays [17]. More recently, 3D printing has become another promising way to prepare ferroelectrets with artificial cavities [21, 22]. (3) Open-porous structures such as ePTFE are fabricated by heating plus accelerated pulling of PTFE rods [23]; in order to prevent the stored charges from leaking from the interface between ePTFE film and electrodes after microplasma-discharge poling, two solid FEP films are usually inserted at the top and bottom of the ePTFE layer to form a sandwich structure [8, 24]. Compared to the widely used cellular-PP ferroelectrets that can only withstand 60 °C [25], ePTFE-based sandwich ferroelectrets offer higher piezoelectric coefficients (of up to 400 pC/N) with superior thermal and long-term stability due to the good charge stability of porous PTFE films [24, 26]. Moreover, additional bipolar ions can be prefilled into the open pores of ePTFE and then separated during dielectric-barrier discharges (DBDs), resulting in much higher piezoelectricity [27]. Therefore, ePTFE-based ferroelectrets of open-porous material systems with high thermal stability are quite attractive compared to other ferroelectrets.

The influence of film geometry and breakdown field on ePTFE-based sandwich ferroelectrets has been successfully modeled [20, 28] under the premise that positive and negative charges are trapped at opposite sides of inner voids in ePTFE and at the interfaces between ePTFE and solid FEP [29]. However, the position of trapped charges was merely inferred from the charge motion during thermally stimulated discharge of the ePTFE-based sandwiches [24]. Until now, there has only been limited or indirect evidence for the location of internal charges. It was also shown that multi-layer laminated ePTFE-based ferroelectrets, e.g. FEP/ePTFE/FEP stacks, should have a better piezoelectric performance due to enhanced macro-dipole moments and higher overall elastic compliance [30]. However, direct and detailed information on spatial charge distributions in fibrous dielectrics [31] is difficult to find, in part due to the complexity of multi-layer laminated structures such as ePTFE-based ferroelectrets with spatially varying acoustic and electric properties [32]. Identifying more or less exact charge positions is essential for quantitatively assessing macroscopic dipole moments and the piezoelectricity of ePTFEbased ferroelectrets.

The Pulsed Electro Acoustic (PEA) technique is one of the most widely used methods for nondestructively measuring space charges and their distributions [33]. The principle is that the movement of space charge in dielectrics under the action of an external electric pulse is transmitted to a piezoelectric sensor as an acoustic pulse. The position and density of the space charge can then be obtained from the electrical signal recorded by means of the piezoelectric sensor [33–35]. The location and amount of space charges trapped in ePTFE-based ferroelectrets can thus be visually characterized with the PEA method to provide essential information needed to quantitatively study the macroscopic dipole moment (the product of charge and separation distance) for analyzing, understanding and further optimizing the piezoelectric performance of ePTFE-based ferroelectrets.

In this paper, the charge distributions in ePTFE-based ferroelectrets with FEP/ePTFE/FEP or FEP/ePTFE/FEP/ePTFE/FEP stacking sequences were mapped by means of the PEA method. The corresponding ferroelectric hysteresis loops were obtained by displacement-*versus*-electric-field (*D-E*) measurements, and the piezoelectric performance of the two structures were analyzed based on the charge-spring model.

2. Experimental section

2.1. Fabrication and characterization of ePTFE-based laminated structures

Expanded PTFE (ePTFE) with the original thickness of about 20 μ m and an average pore size of 3 μ m was supplied by BHA Altair, LLC, a Parker Hannifin Company. It should be noted that all pores are interconnected inside the ePTFE film, and the pore size refers to the size of the holes surrounded by fiber filaments. FEP film with the thickness of 12.5 μ m was purchased from Goodfellow Corp. The films were laminated together at 285 °C under 5 kN force for 1 h in a Carver Laboratory hot press. A detailed description about the hot-pressing process can be found in the literature [30]. Considering the reduction of the sample thickness during hot pressing and the requirement of a sample thickness between 50 and 200 μ m for PEA measurements, the FEP/ePTFE/FEP stack was prepared by fusing a sequential stack of 2 layers of FEP plus 4 layers of ePTFE plus 2 layers of FEP together, and the FEP/ePTFE/FEP/ePTFE/FEP structure was obtained by stacking and fusing 2 layers of FEP plus 4 layers of ePTFE plus 2 layers of FEP plus 4 layers of ePTFE plus 2 layers of FEP, respectively. The micromorphology of the laminated structures was characterized by means of a ThermoFisher Verios SEM.

2.2. Corona-poling process

Laminated stacks, FEP/ePTFE/FEP and FEP/ePTFE/FEP/ePTFE/FEP, which are designated as F/e/F and F/e/F/e/F, respectively, for brevity in the following, were charged by means of DBDs in a corona-poling process. The film stack was corona-charged for 5 min at a distance of 5 cm below the corona needle tip biased at a voltage of +20 kV, during which bipolar charges were generated by Paschen breakdown of the air inside ePTFE under the high electric field, and macro-dipoles were formed by the charges trapped in the large overall pore across the ePTFE layer. Thus, piezoelectricity was enabled by the macro-dipoles, the dipole moment of which changes upon compression or rarefaction.

2.3. Pulsed Electroacoustic (PEA) measurement

The two sides of the samples were first metallized through sputter coating with 60%/40% gold/palladium. The semiconductive electrode of the PEA setup was coated with a thin layer of silicone oil then connected with the sample for a better acoustic impedance matching. A voltage of 350 V with a pulse width of 10 ns and a rise time of 1 ns was utilized to excite the acoustic wave. A 9 μ m PVDF sensor with a back absorber was employed to convert the acoustic wave into an electrical signal recorded on a Tektronix DPO5034 oscilloscope. Each ePTFE-based laminated structure was tested before and after corona poling, and the distribution of charges trapped during the poling process was obtained by comparing the two PEA results.

2.4. Characterization of piezoelectricity

The ferroelectric hysteresis effect of ferroelectrets was recorded in a modified Sawyer–Tower circuit with a specific waveform consisting of two positive, two negative and then two positive sinusoidal semi-cycles in sequence [30, 36]. The duration of the overall waveform with six semi-cycles is 3 s. Charges obtained during the first semi-cycles at each polarity are contributed by the sample capacitance, conductance and ferroelectric polarization, while the second semi-cycles of each pair only show the contributions of conductance and capacitance. By subtracting the charges obtained during the second three semi-cycles from those found during the first three semi-cycles and smoothing the curve, remnant charges caused by the ferroelectric polarization, as well as the final *D-E* hysteresis loop, can be obtained.

A PM3500 Berlincourt meter from KCF Technologies was used to measure the d_{33} coefficient of the ePTFE-based laminated structures after poling. The applied force was 0.25 N and the frequency was 110 Hz. Because the films were too soft for the hard probe, two aluminum sheets were utilized as electrodes on the top and bottom of the film stack during measurement.

3. Results and discussion

3.1. Charge distributions of multilayer ePTFE-based ferroelectrets

Figure 1 shows (a) the SEM cross-section image of the FEP/ePTFE/FEP structure and (b, c) the corresponding spacecharge distribution along the thickness direction obtained by use of the PEA method side-by-side. For the chargedistribution image in figure 1(b), the vertical axis indicates the normalized sample thickness, where zero and one represent the cathode and anode positions, respectively. The horizontal axis indicates the measuring time. The color bar on the right codes the space-charge density in C m⁻³; in addition, a 2D plot of charge density vs. position at the end of the measurement (at 15 s) is shown in figure 1(c). One negative and one positive charge band can be observed in the space-charge distribution across the thickness. Comparing figures 1(a) and (b), the charge bands are found at the interfaces between FEP and ePTFE. The charge densities might have been reduced during sputter coating of the open-porous sample structure, and the observed widths of the charge bands could be affected by the acoustic impedance-difference between FEP and ePTFE; [32] however, the charge-density map clearly shows—as far as we know, for the first time—the spatial distribution and the polarity of the charges: Negative and positive charges are well separated and trapped at the top and bottom ePTFE/FEP interfaces, respectively, to form one macro-dipole across the threelayer film sandwich. The essential role of the solid sealing films (FEP) for the open-porous ferroelectrets is thus demon-

In order to further study the formation of macro-dipoles in laminated multi-layer ePTFE-based ferroelectrets, the charge in the FEP/ePTFE/FEP/ePTFE/FEP stack was also mapped.

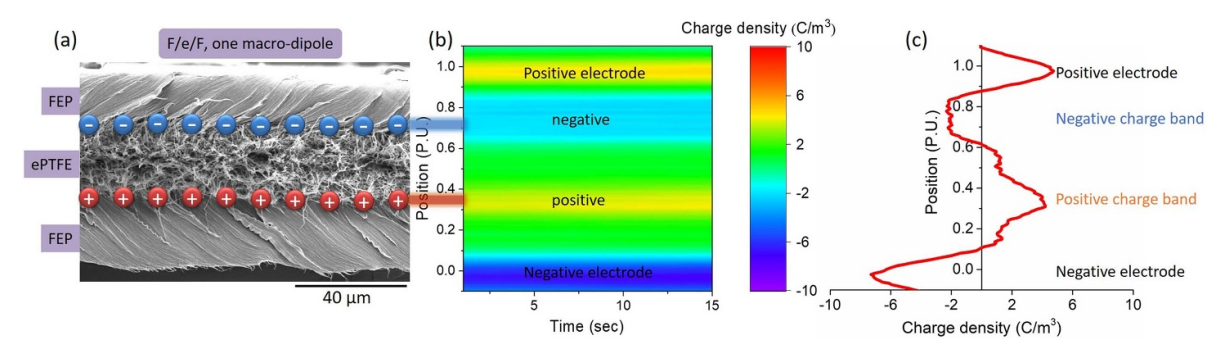


Figure 1. (a) SEM image of the cross-section of an FEP/ePTFE/FEP stack, (b) color-coded charge-density map, and (c) 2D plot of the charge distribution, as obtained by use of the PEA method.

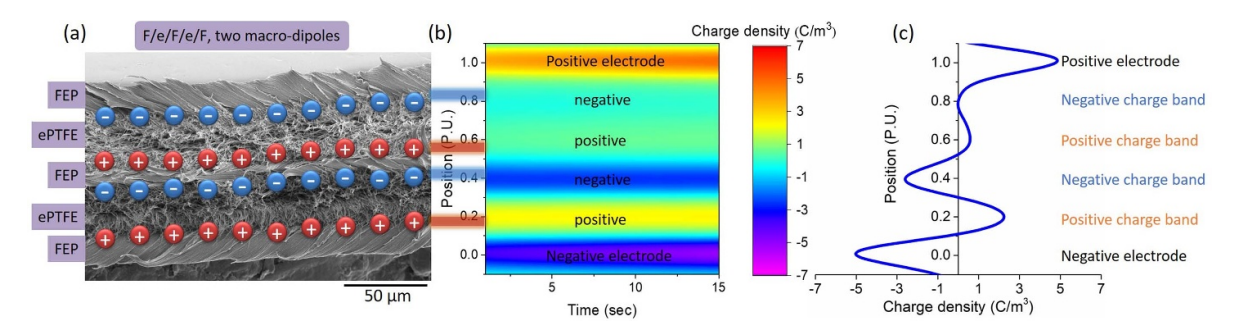


Figure 2. (a) Cross-sectional SEM image of an FEP/ePTFE/FEP/ePTFE/FEP stack, (b) color-coded map and (c) 2D plot of the charge distribution obtained by use of the PEA method.

Its cross-sectional SEM image and the measured spacecharge distribution are shown side-by-side in figure 2, and figure 2(c) shows a 2D plot of charge density vs. position at 15 s. In this case, two negative and two positive charge bands can be observed across the sample. In comparison with the SEM cross-sectional image of the sandwich film, the four color-coded bands of space charge correspond very well to the four ePTFE/FEP interfaces within the laminated ePTFE-based ferroelectret. One negative and one positive charge band together form one macro-dipole, and overall, two macro-dipoles are stacked in series along the thickness direction. All charge layers in the five-layer ePTFE-based ferroelectret are trapped at the respective interfaces between FEP and ePTFE, and the two sides of the FEP film at the center of the stack carry charges of opposite polarity.

As shown in figure 2(b), the charge densities of the bottom macro-dipole appear to be higher than those of the upper macro-dipole. This observation may essentially be an artifact caused by stronger attenuation of the acoustic waves during propagation to the PVDF sensor at the bottom from the charges near the top electrode [37].

Therefore, the same FEP/ePTFE/FEP/ePTFE/FEP ferroelectret film has been measured again with the PVDF sensor at the top (figure 3(b)), and the result is directly compared to the earlier measurement with the PVDF sensor at the bottom (figure 3(a)). The space-charge distribution from the second measurement shows that there are still four charge bands across the thickness of the ferroelectret film, but now the upper two bands are more prominent. Overall, the charge densities in the four bands of figure 3(b) are not as high as those in figure 3(a). This is because the ferroelectret film had been re-metallized before the second measurement, which led to a further charge loss during sputter coating. Another possible reason for the reduced charge densities is the fact that the second measurement was performed 10 d after the first one so that the internal charges may have partially decayed due to thermal stress. Nevertheless, the more prominent upper macro-dipole in figure 3(b) confirms attenuation of the acoustic signal that propagates towards the PVDF sensor. Thus, it can be assumed that the spatial distribution of the charge density is in reality more uniform and that the calibration of the PEA setup needs to be improved for heterogeneous samples, with consideration of the acoustic impedancedifference of the materials in the sample. Considering the film thickness, the poling field across the sample stack should initially be quite uniform, and the macro-dipoles in the FEP/ePTFE/FEP/ePTFE/FEP stack should not exhibit a significant difference.

3.2. Piezoelectric performance of the ePTFE-based ferroelectrets

Figures 4(a) and (b) show the displacement-*versus*-electric-field (*D-E*) loops of the two stacks, F/e/F and F/e/F/e/F, respectively. The *D-E* curves of both stacks are essentially

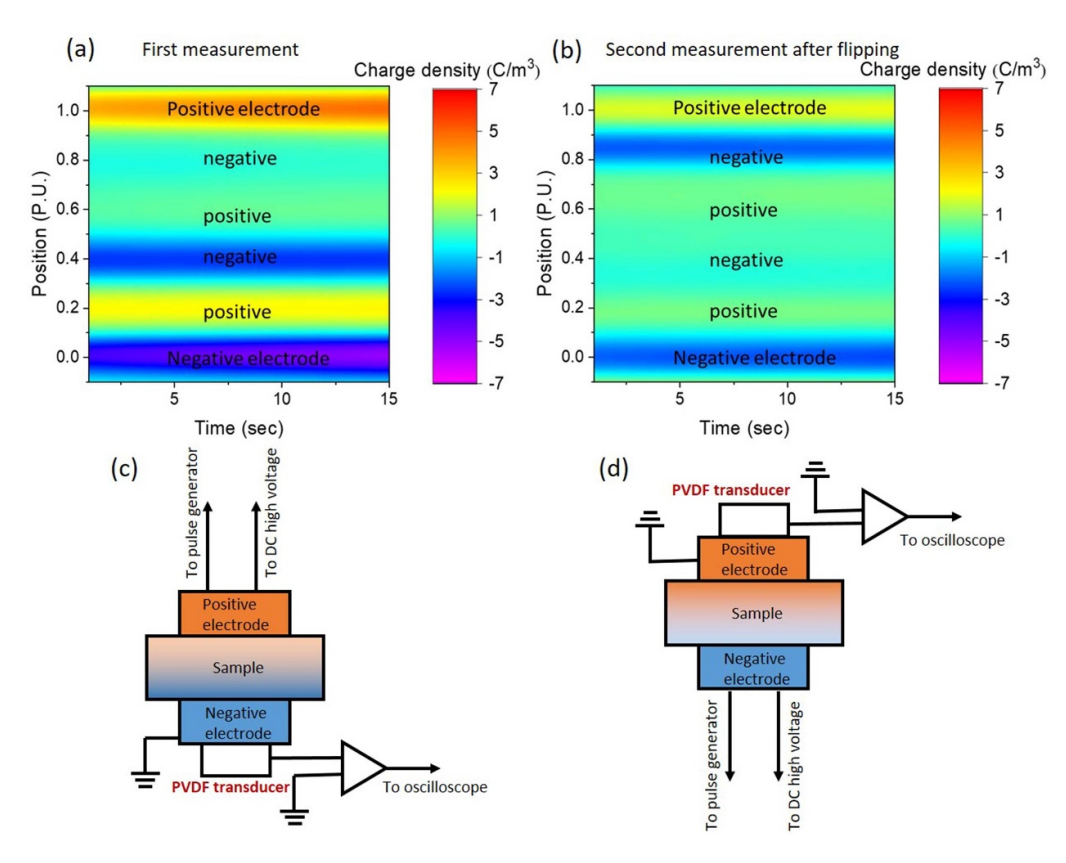


Figure 3. Charge distribution in an FEP/ePTFE/FEP/ePTFE/FEP stack measured (a) with the PVDF transducer at the bottom (c) and (b) with the PVDF transducer on top (d).

parallelograms, with evidently ferroelectric-hysteresis behavior. The intercept value at zero electric field is the remnant charge density that should indicate the remnant polarization in the ferroelectret films. After applying an electric field of 100 kV mm⁻¹, the remnant charge density of the F/e/F/e/F structure is about two times that of the F/e/F structure. It should be noted that there are two macro-dipoles in the F/e/F stack (figure 2), while there is only one in the F/e/F stack (figure 1). Thus, the remnant polarization of the laminated ferroelectrets is directly related to the number of macro-dipoles.

According to the charge-spring model, the piezoelectric coefficient of a ferroelectret can be estimated as the sum of the ratio between the remnant polarization and the elastic modulus of the dipole layer and the matrix layer, respectively, where the matrix-related term (dipole-density effect) is negative, while the dipole-related term (dipole-moment effect) is positive [38]

$$d_{33} \approx -\frac{P_3}{Y_{\rm M}} + \frac{P_3}{Y_{\rm D}};$$
 (1)

here, P_3 is the polarization along the thickness direction, and $Y_{\rm M}$ and $Y_{\rm D}$ are the elastic moduli of the matrix phase and the dipole phase, respectively. Since the ratio of the elastic moduli between FEP and ePTFE is quite large (>100) [28], it can be assumed that essentially only the dipole phase is compressible so that the negative matrix term can be neglected. Thus, the

piezoelectric d_{33} coefficient of the layered ferroelectret can be predicted as the ratio of P_3 and Y_D .

As we only know the resulting piezoelectric coefficients for the three- and five-layer stacks (150 pC/N and 200 pC/N, respectively) and the remnant polarizations in both cases $(0.75 \ \mu\text{C cm}^{-2} \text{ from figure 4(a) and } 1.6 \ \mu\text{C cm}^{-2} \text{ from}$ figure 4(b), respectively), we can estimate the respective elastic moduli as 50 MPa for the F/e/F stack and 80 MPa for the F/e/F/e/F stack, respectively. The two moduli are higher by a factor of 2.5 and 4, respectively, than the elastic-modulus value of a single ePTFE layer reported in the literature as 20 MPa [39]. The differences are probably caused—at least to a large extent-by the strong reduction of the ePTFE porosity during hot pressing and by the additional hardening of the fivelayer stack due to the central FEP layer and the fusing of all the individual films into double layers. The influence of such hardening effects can probably be avoided or at least reduced by starting from softer ePTFE material, by using single thicker films instead of double films in the stacks, and by employing a gentler lamination process. If all other parameters would remain roughly the same, significantly higher d_{33} coefficients of up to 400 and 800 pC/N, respectively, could be expected for the two stacks [27]. Thus, the piezoelectric performance of ePTFE-based ferroelectrets is mainly affected by the number of internal macro-dipoles in the stack and by Young's modulus of the structure which is mainly determined by the much softer ePTFE films.

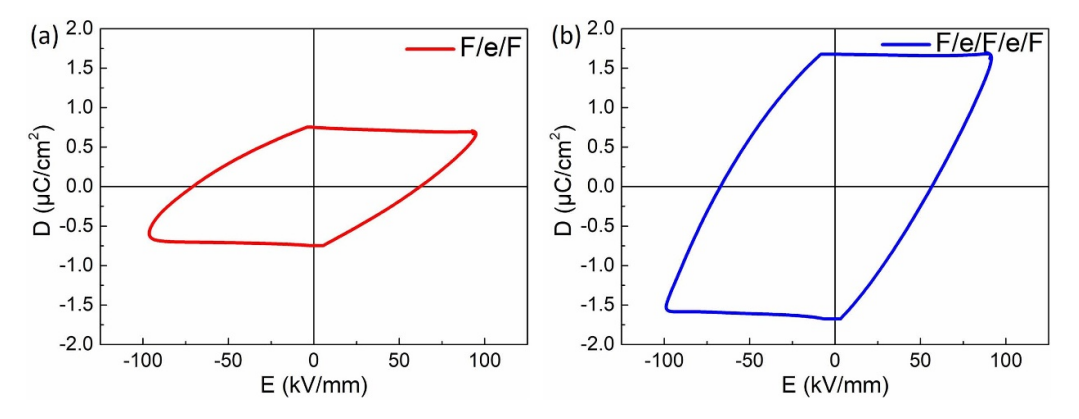


Figure 4. *D-E* hysteresis loops of the ferroelectret film stacks with FEP/ePTFE/FEP (left) and FEP/ePTFE/FEP/ePTFE/FEP (right) layer sequences.

4. Conclusions

For the first time, the spatial charge distributions in ePTFE-based ferroelectrets were probed by use of the PEA method. On FEP/ePTFE/FEP and FEP/ePTFE/FEP/ePTFE/FEP ferroelectret stacks, the influences of the number of macro-dipoles on the remnant polarization and on the overall piezoelectric performance of the ferroelectret stacks could be elucidated as follows:

- 1) According to the charge distributions revealed in the PEA measurements, negative and positive charges are separated and trapped at the two FEP/ePTFE interfaces of an ePTFE film to form a macro-dipole across the compressible ePTFE in the thickness direction of the FEP/ePTFE/FEP structure. With respect to the FEP/ePTFE/FEP/ePTFE/FEP stacking configuration, it is interesting to note that heterocharges of opposite polarities were trapped in alternating order at the FEP/ePTFE interfaces to form two macro-dipoles, electrically connected in series to yield a favorable larger overall polarization in the stack.
- 2) The remnant polarization seen in the *D-E* loop of the FEP/ePTFE/FEP/ePTFE/FEP configuration is approximately two times that of the FEP/ePTFE/FEP structure, due to the series connection of two macro-dipoles. The piezoelectric coefficient of the ePTFE-based ferroelectrets is thus enhanced, with an experimental *d*₃₃ value of 200 pC/N for the FEP/ePTFE/FEP/ePTFE/FEP stacking configuration. By use of optimal materials and under optimal processing conditions, significantly higher *d*₃₃ values might be achievable.

Data availability statement

All data that support the findings of this study are included within the article (and any supplementary files).

Acknowledgments

The authors are very grateful to Professor George Rossetti for providing the PM3500 d_{33} meter for the piezoelectrical measurement and to BHA Altair, LLC, a Parker Hannifin Company, for providing the expanded PTFE films employed in this study.

ORCID iDs

Ningzhen Wang https://orcid.org/0000-0002-1263-7266
Robert Daniels https://orcid.org/0000-0003-1114-5515
Jindong Huo https://orcid.org/0000-0003-3725-9035
Reimund Gerhard https://orcid.org/0000-0002-1306-2249
Yang Cao https://orcid.org/0000-0001-7034-2792

References

- Fan F R, Tang W and Wang Z L 2016 Flexible nanogenerators for energy harvesting and self-powered electronics Adv. Mater. 28 4283
- [2] Qi Y and McAlpine M C 2010 Nanotechnology-enabled flexible and biocompatible energy harvesting *Energy Environ. Sci.* 3 1275
- [3] Yilmaz T, Foster R and Hao Y 2010 Detecting vital signs with wearable wireless sensors Sensors 10 10837
- [4] Chen G, Li Y, Bick M and Chen J 2020 Smart textiles for electricity generation *Chem. Rev.* **120** 3668
- [5] Liu H, Zhong J, Lee C, Lee S and Lin L 2018 A comprehensive review on piezoelectric energy harvesting technology: materials, mechanisms, and applications *Appl. Phys. Rev.* 5 41306
- [6] Kacprzyk R, Motyl E, Gajewsk J B and Paternak A 1995 Piezoelectric properties of nonuniform electrets *J. Electrost.* 35 161
- [7] Hillenbrand J and Sessler G M 2000 Piezoelectricity in cellular electret films *IEEE Trans. Dielec. Electr. Insul.* **7** 537
- [8] Qiu X 2016 Polymer electrets and ferroelectrets as EAPs: materials *Electromechanically Active Polymers. A Concise Reference* ed F Carpi (Springer) ch 30, p 561
- [9] Lu L, Ding W, Liu J and Yang B 2020 Flexible PVDF based piezoelectric nanogenerators Nano Energy 78 105251

- [10] Zhang X, von Seggern H, Sessler G M and Kupnik M 2020 Mechanical energy harvesting with ferroelectrets *IEEE Electr. Insul. Mag.* 36 47
- [11] Zhang Y, Bowen C R, Ghosh S K, Mandal D, Khanbareh H, Arafa M and Wan C 2019 Ferroelectret materials and devices for energy harvesting applications *Nano Energy* 57 118
- [12] Habib M, Lantgios I and Hornbostel K 2022 A review of ceramic, polymer and composite piezoelectric materials J. Phys. D: Appl. Phys. 55 423002
- [13] Wegener M, Wirges W, Fohlmeister J, Tiersch B and Gerhard-Multhaupt R 2004 Two-step inflation of cellular polypropylene films: void-thickness increase and enhanced electromechanical properties J. Phys. D: Appl. Phys. 37 623
- [14] Qiu X, Fang P, Mellinger A, Altafim R A P, Wirges W, Gidion G and Rychkov D 2023 Ferroelectrets: heterogenous polymer electrets with high piezoelectric sensitivity for transducers J. Adv. Dielectr. 13 2341009
- [15] Nakayama M, Uenaka Y, Kataoka S, Oda Y, Yamamoto K and Tajitsu Y 2009 Piezoelectricity of ferroelectret porous polyethylene thin film *Jpn. J. Appl. Phys.* 48 9
- [16] Hu H, Zhu W, Li D and Qu Y 2021 Waterproof and low-cost piezoelectrets with high piezoelectric responses J. Phys. D: Appl. Phys. 54 415502
- [17] Li Y and Zeng C 2013 Low-temperature CO₂-assisted assembly of cyclic olefin copolymer ferroelectrets of high piezoelectricity and thermal stability *Macromol. Chem. Phys.* 214 2733
- [18] Zhang X, Pondrom P, Sessler G M and Ma X 2018 Ferroelectret nanogenerator with large transverse piezoelectric activity *Nano Energy* 50 52
- [19] Zhou L, Zhang F, Ma X and Zhang X 2023 Influence of soft x-ray and ultraviolet irradiations on sensitivity of sensors made with piezoelectret films J. Phys. D: Appl. Phys. 56 435304
- [20] Zhukov S, Fedosov S and von Seggern H 2011 Piezoelectrets from sandwiched porous polytetrafluoroethylene (ePTFE) films: influence of porosity and geometry on charging properties J. Phys. D: Appl. Phys. 44 105501
- [21] Assagra Y A O, Altafim R A P, Do Carmo J P, Altafim R A C, Rychkov D, Wirges W and Gerhard R 2020 A new route to piezo-polymer transducers: 3D printing of polypropylene ferroelectrets *IEEE Trans. Dielec. Electr. Insul.* 27 1668
- [22] Kierzewski I, Bedair S S, Hanrahan B, Tsang H, Hu L and Lazarus N 2020 Adding an electroactive response to 3D printed materials: printing a piezoelectret *Addit. Manuf.* 31 100963
- [23] Gore-Tex Fabrics Technical Information (available at: www. gore.com) (Accessed 5 January 2024)
- [24] Hu Z and von Seggern H 2006 Breakdown-induced polarization buildup in porous fluoropolymer sandwiches: a thermally stable piezoelectret *J. Appl. Phys.* **99** 24102

- [25] Wu N, Cheng X, Zhong Q, Zhong J, Li W, Wang B, Hu B and Zhou J 2015 Cellular polypropylene piezoelectret for human body energy harvesting and health monitoring Adv. Funct. Mater. 25 4788
- [26] Xia Z, Wedel A and Danz R 2003 Charge storage and its dynamics in porous polytetrafluoroethylene (PTFE) film electrets *IEEE Trans. Dielec. Electr. Insul.* 10 102
- [27] Wang N, van Turnhout J, Daniels R, Wu C, Huo J, Gerhard R, Sotzing G A and Cao Y 2022 Ion-boosting the charge density and piezoelectric response of ferroelectrets to amazingly high levels ACS Appl. Mater. Interfaces 14 42705
- [28] von Seggern H, Zhukov S and Fedosov S 2011 Importance of geometry and breakdown field on the piezoelectric d₃₃ coefficient of corona charged ferroelectret sandwiches *IEEE Trans. Dielec. Electr. Insul.* 18 49
- [29] Sessler G M and Hillenbrand J 1999 Electromechanical response of cellular electret films 10th Int. Symp. on Electrets (ISE 10) vol 99 p 261
- [30] Wang N, Daniels R, Connelly L, Sotzing M, Wu C, Gerhard R, Sotzing G A and Cao Y 2021 All-organic flexible ferroelectret nanogenerator with fabric-based electrodes for self-powered body area networks *Small* 17 2103161
- [31] Thakur R, Das D, Das A and Reddy C C 2015 Spatial charge distribution in fibrous dielectrics *J. Electrost.* **76** 1
- [32] Bodega R, Morshuis P H F and Smit J J 2006 Space charge measurements on multi-dielectrics by means of the pulsed electroacoustic method *IEEE Trans. Dielec. Electr. Insul.* 13 272
- [33] Uehara H, Li Z, Chen Q, Montanari G C and Cao Y 2017 Space charge behavior under thermal gradient in cross-linked polyethylene and ethylene-propylene rubber Sens. Mater. 29 1199
- [34] Wu C, Arab M, Ronzello J and Cao Y 2021 Charge transport dynamics and space charge accumulation in XLPE composites with 2D platelet fillers for HVDC cable insulation *IEEE Trans. Dielec. Electr. Insul.* 28 3
- [35] Arab Baferani M, Wu C and Cao Y 2022 Charge transport and space charge dynamics in EPDM/2D-nanoclay composite dielectrics Compos. Sci. Technol. 219 109241
- [36] Qiu X, Holländer L, Wirges W, Gerhard R and Cury Basso H 2013 Direct hysteresis measurements on ferroelectret films by means of a modified Sawyer–Tower circuit *J. Appl. Phys.* 113 224106
- [37] Nga Vu T T, Berquez L and Teyssedre G 2018 Space charge measurement by electroacoustic method: impact of acoustic properties of materials on the response for different geometries *Int. J. Electr. Eng. Inform.* 10 631
- [38] Gerhard R 2014 A matter of attraction: electric charges localized on dielectric polymers enable electromechanical transduction *Annual Report* (IEEE CEIDP) pp 1–10
- [39] Mohd Hidzir N, Mohd Radzali N A, Abdul Rahman I and Shamsudin S A 2020 Gamma irradiation-induced grafting of 2-hydroxyethyl methacrylate (HEMA) onto ePTFE for implant applications *Nucl. Eng. Technol.* 52 2320